Two- and Three-Directional Synthesis by 3-7MCRs of Novel (Imidazolidine/Thiazolidine)-2,4-Diones: Characterization, Antibacterial, Anticonvulsant and Molecular Docking Investigation

Hadiseh Yazdani Nyaki
University of Guilan
Nosrat O. Mahmoodi (mahmoodi@guilan.ac.ir)
University of Guilan
Hossein Taherpour Nahzomi
Payame Noor University
Esmaeel Panahi Kokhdan
Yasuj University of Medical Sciences

Research Article

Keywords: Two and three directions synthesis, Antibacterial activity, Molecular docking, Imidazolidine-2,4-dione, Thiazolidine-2,4-dione, Anticonvulsant activity

Posted Date: January 31st, 2023

DOI: https://doi.org/10.21203/rs.3.rs-2517541/v1

Abstract

A variety of new compounds containing two or three biologically active nuclei of imidazolidine-2,4-dione and thiazolidine-2,4-dione (TZD) via optimization two and three directional 3 and 4MCRs Knoevenagel condensation (**method A**) and two and three directional 5 and 7 MCRs Bucherer-Bergs (**method B**). The structure of these derivatives was confirmed by FT-IR, ^{1}HNMR, ^{13}CNMR, and Elemental analysis. To evaluate the anticonvulsant activity of these derivatives, all the compounds were subjected to molecular docking studies for Anticonvulsant Drug Binding (ADB) to the Voltage-Gated Sodium Channel Inner Pore (VGCIP). The in silico molecular docking study results showed that molecules **5c**, **9**, **7**, and **10** among the synthesized compounds have the lowest docking score which shows the highest combined desire for the channel and have a good affinity toward the active pocket, thus, they may be considered good anticonvulsant agents. Also, to evaluate the antibacterial properties of these derivatives, they underwent molecular docking studies with four bacterial proteins. Gram-positive bacteria such as *B. anthracis* (PDB ID: 3TYE) and *S. aureus* (PDB ID: 3ACX) and gram-negative bacteria *E. coli* (PDB ID: 1AB4) and *P. aeruginosa* (PDB ID: 5U39). The most significant overall score has been obtained for *S. aureus* (PDB ID: 3ACX) bacteria. A combination of **10** displays strong antibacterial activity against two gram-positive bacterial and compounds **4a** and **7** with gram-negative proteins bacterial. The highest binding affinity is related to compound **7** for gram-negative *P. aeruginosa* (PDB ID: 5U39) bacterial proteins. The antibacterial properties of these derivatives were as well experimentally investigated.

1. Introduction

The examination of superior structures in drug discovery has gained increasing popularity in pharmaceutical chemistry over the years. Because heterocyclic rings have significant biological activities, studies on these compounds have increased significantly [1–4].

Today, derivatives containing imidazolidine-2,4-dione and thiazolidine-2,4-dione derivatives have been extensively studied and represent a wide range of pharmacological activities, including anti-convulsant, anti-bacterial, and anti-epileptic, anti-tuberculosis, anti-tumor, anti-diabetic, anti-inflammatory, analgesic, anti-seizure, anti-viral, anti-HIV, anti-depressant and molecular modeling study [5–12]. Figure 1 indicates famous clinical drugs including biological imidazoline-2,4-dione and thiazolidine-2,4-dione rings.

Compounds with two and three rings of imidazolidine-2,4-dione and thiazolidine-2,4-dione have been synthesized via two and three directions strategy as well, and in addition their therapeutic properties have found some useful industrial applications [13–20]. In 2006, Christian V. Stevens and colleagues synthesized a compound containing two IMID rings with the application as a fire retardant of some polymers [21]. In 2012, V. Haridas and colleagues through the synthesis of compounds bearing two IMID rings were able to prepare fibers representing antimicrobial properties as well as industrial usage [22]. Furthermore, in 2016, Alireza Salimi Beni and colleagues synthesized compounds containing two TZD rings that are color-sensitive in solar cells for photovoltaic devices [23]. In 2018, Asok K. Mallik and colleagues synthesized a compound containing two TZD rings with a sensor effect to detect metal ions

[24]. A noteworthy feature of compounds involving imidazolidine-2, 4-dione ring is their anticonvulsant activity. A Convulsant is usually defined as a sudden alteration of behavior due to a temporary change in the electrical functioning of the brain. Normally, the brain continuously generates tiny electrical impulses in an orderly pattern [25,26]. Amongst the compounds including imidazolidine-2,4-dione moiety such as phenytoin Fig. 1 is a well-known usage in the treatment of sudden epileptic illness. The mechanism of action of this drug is that it controls the voltage-dependent Na-channels of neurons and the influx of Ca from nerve cells, increasing the normal seizure threshold and inhibiting seizure activity [27,28].

Also, another notable feature of compounds involving of compounds containing imidazolidine /thiazolidine (2,4)-dione rings is the antibacterial properties of these compounds against various types of gram-positive and gram-negative bacteria [29–34]. Accordingly, in this study, new compounds were developed that have two or three active rings of imidazolidine and thiazolidine. Molecular docking is used as an important tool for understanding the interactions between a drug-containing combination and a sufficient level for its potential use in therapy. This method could be a good perspective for new compounds in various activities, especially as catalysts, drug carriers, or in the treatment of cancer to study the interaction with different enzymes [35–40].

Here, the two and three directions synthesis strategy as well the identification of (bis & tris) imidazolidine/thiazolidine(2,4)-dione target compounds was described. The binding energy of the amino acids forming the proteins of gram-positive and gram-negative bacteria was investigated by the molecular docking method. In the other efforts bacterial experiments were as well performed to verify the results. Furthermore, the bond formation energy on amino acids affects the voltage characteristics of the Na-channel in comparison with the anticonvulsant activity of phenytoin was investigated and their factors evaluated.

2. Result And Discussion

2.1. *Chemistry*

Targeting synthesis (5Z,5'Z)-5,5'-(1,4-phenylenebis(methaneylylidene))bis(thiazolidine-2,4-dione) 1 via two directions synthesis, **Method A**, based on the one-pot Knoevenagel 3MCR in EtOH as a solvent, Piperidine as a catalyst was used (Scheme 1**)**. In other efforts one-pot 5MCRs as a two directions synthesis (modified Bucherer–Bergs reaction) utilizing KCN, $(NH_4)_2CO_3$ and 50% EtOH as a solvent was used **Method B (**Scheme 1**) that** lead to the production of 5,5'-(1,4-Phenylene)bis(imidazolidine-2,4-dione) 2.

The structure of TZD-derivative **1** was characterized by FT-IR, ^{1}HNMR, ^{13}CNMR and Elemental analysis (C, H, O, N and S). The formation of TZD-derivative was confirmed by the appearance of a sharp singlet for NH-TZD protons at 12.73 ppm and a singlet for -C = CH protons at 8.20 ppm in ^{1}HNMR spectra followed by the presence of peaks 3133 cm^{-1} (NH_{str}), 1748 – 1699 cm^{-1} (C = O_{str}) and 1601 cm^{-1} (-CH = Cstr), in the FT-IR spectrum.

The synthesis of the **2** [41] was obtained according to **method B (**Scheme 1**)** as a cream-powder with a high yield. The structure of **2** was confirmed by FT-IR, ^{1}HNMR, ^{13}CNMR, and Elemental analysis (C, H, O, and N). In ^{1}HNMR at 10.92 and 9.03 ppm two single peaks for NH-IMID protons and 5.82 ppm for -CH-NH was revealed. The FT-IR spectrum shows two peaks at 3295, 3218 cm^{-1} (NH_{str}), 1779 – 1714 cm^{-1} (C = O_{str}) recognized to the structure of this compound with imidazolidine-2,4-dione moiety.

For synthesis of **4(a-b)** and **5(a-c)**, which are the constituents of bis-thiazolidine / imidazolidine (2,4)-dione, the precursors of bis-aldehydes **3(a-c)** were first synthesized (Scheme 2).

Accordingly, using 2 Equiv. of **2** or 4-hydroxybenzaldehydes and 1 Equiv. of dihaloalkane or dihalobenzyl in DMF using K_2CO_3 were completed according to the two directional-S_N2 reaction [42], and the final product of bis-compounds was obtained. The synthesized bis-compounds **4(a-b)** and **5(a-c)** are new derivatives of the bis-imidazolidine/ thiazolidine (2,4)-dione obtained under reflux and specific temperature conditions using **methods A** and **B**. Reaction products precipitate with optimum efficiency without any major by-products.

The precipitates were recrystallized relatively straightforwardly. New synthetic compounds **4(a-b)** and **5(a-c)** were characterized by FT-IR, ^{1}H NMR, ^{13}CNMR and Elemental analysis (C, H, O, N and S) data were within ± 0.4% of the theoretical values. The structure and physical characteristics of the derivatives containing the imidazolidine-2,4-dione ring **4(a-b)** and the derivatives containing the thiazolidine-2,4-dione ring **5(a-c)** are presented in Table 1.

Table1. The structure of the new synthesis products **4(a-b)** and **5(a-c)**

Entry	Structure	M.P (°C)	Color
4a	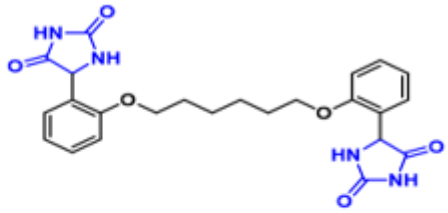	126-128	
4b	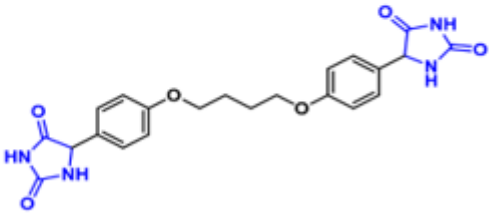	180-182	
5a	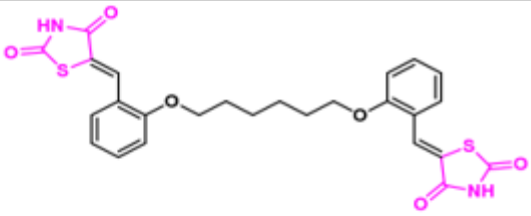	258-260	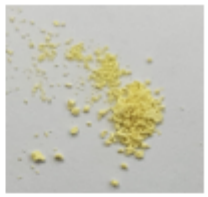
5b	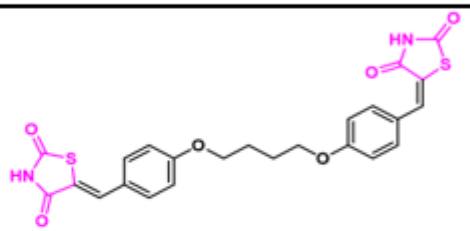	166-168	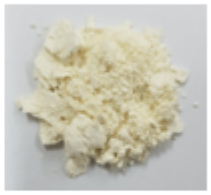
5c	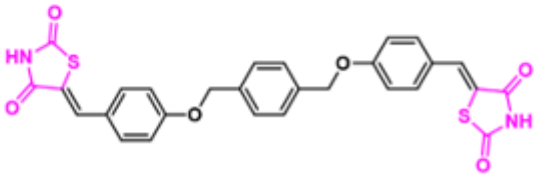	216-218	

Generally, in the FT-IR spectrum, compounds **4(a-b)**, which are members of imidazolidine-2,4-dione derivatives, showed two stretching vibration bands for NH in the range of 3363 – 3218 cm^{-1}. Two Fermi absorption resonance bands in the area of 1779 – 1714 cm^{-1} are related to two C = O stretching bands. The ^{1}H NMR spectra of new compounds were recorded in DMSO-d_6 at 25 ºC.

Given that these compounds have a plane of symmetry, the ^{1}H NMR spectra of **4(a-b)** showed two signals in the range of 12.77–9.03 ppm due to the NH-IMID protons each with an integration intensity equal to one H-atom. Also, the singlet at 5.19 ppm (1H) is typical of the H-benzylic of the imidazolidine-2,4-dione ring.

The FT-IR spectrum of compounds **5(a-c)**, which are members of thiazolidine-2,4-dione derivatives, showed one stretching vibration band for NH in the range of 3235–33107 cm^{-1}. Two different absorption

bands in the area of 1738 – 1689 cm^{-1} are related to two C = O stretching bands and the benzylidene stretching bound -CH = C appeared in the range of 1589–1602 cm^{-1}.

^{1}H NMR spectra of **5(a-c)** were obtained the derivatives of bis-thiazolidine-2,4-dione also have a similar spectrum. The spectrum displayed one sharp singlet peak of about 11.61–12.49 ppm which can be attributed to the NH-TZD. Also, a single peak for -C = CH (H- benzylidene) proton is almost 7.85–9.03 ppm.

In Scheme 3, to prepare the **7** via 3MCR initially **6** [43] according to the modified 3MCR-Bucherer–Bergs which previously described from 4-hydroxy benzophenone was premade. Product **6** is a light yellow powder, was identified by FT-IR, $^{1}HNMR$, $^{13}CNMR$, and Elemental analysis (C, H, O, and N) data.

4-Hydroxy phenytoin **6**, in the FT-IR spectrum, shows two peaks 3265, 3147 cm^{-1} (NH_{str}), > 3000 broad peak (O-H_{str}), and 1725, 1630 cm^{-1} (C = O_{str}). $^{1}HNMR$ spectra was recorded in DMSO-*d6* at 25 ºC. This spectrum shows at 11.00 and 10.45 ppm two single peaks for NHs-IMID protons and a single peak at 9.17 ppm for OH. The target **7** was synthesized using 2 Equiv. **6**, and 1 Equiv. dichlorobenzene in DMF, using K_2CO_3 through a one-pot 3MCR two-directional-S_N2 mechanism, with a relatively reasonable yield of 7 as a pink powder product, as shown in Scheme 3. Compound **7** was identified by FT-IR, $^{1}HNMR$, $^{13}CNMR$, and Elemental analysis (C, H, O, and N) data were within ± 0.4% of the theoretical values.

To identify the structure of the **7**, FT-IR spectrum shows a peak of 3281 cm^{-1} (NH_{str}), the broad peak corresponding to (O-H_{str}) has been eliminated, the two peaks 2931, 2872 cm^{-1} (C-$H_{\text{aliphatic str}}$) and 1773, 1713 cm^{-1} (C = $O_{\text{Fermi str}}$).

$^{1}HNMR$ spectra was recorded in DMSO-d_6 at 25 ºC, showed two single peaks for NHs-IMID protons at 11.01 and 10.66 ppm and a single peak for (O-CH_2) at 5.31 ppm related to –CH_2 linker. In addition, a single peak for OH has been eliminated and a new peak appears in the aliphatic region which is a significant reason to confirm that the binding of the two molecules **6** was completed through 1,4-bis(chloromethyl)benzene, and **7** was achieved. According to Scheme 4, Tris-aldehyde **8** first was synthesized according to the previously reported procedure [44,45]. The tripod product **10** [46] was completed via three directional 4MCR following **method A**. Tripod **10** is a yellow powder with a good yield as a tris-thiazolidine-2,4-dione derivatives.

In other efforts, tripod **9** was synthesized from corresponding premade **8** as a cream product with a reasonable yield via three directional 7MCR following **method B** (Scheme 4**)**. The structure of **9** was identified by FT-IR, $^{1}HNMR$, $^{13}CNMR$, and Elemental analysis (C, H, O, and N) data were within ± 0.4% of the theoretical values. Tripod 9 with a imidazolidine-2,4-dione moieties indicates the existence of two NH groups in FT-IR, two peaks at 3327, 3193 cm^{-1} (NH_{str}), two peaks at 1733, 1671 cm^{-1} (C = O_{str}). **9** was dissolved very well in DMSO-d_6 at 25 ºC and $^{1}HNMR$ spectra showed two single peaks for NHs-IMID protons at 11.19 and 10.71 ppm.

2.2. *Molecular Docking Study for Antibacterial Effect*

To study and investigate the probable binding affinity and antibacterial effect of the synthesized molecules the docking simulations in active sites of four target proteins of C(30) carotenoid dehydrosqualene synthase of *S. aureus* (PDB ID: 3ACX), Gyrase A of *E. coli* (PDB ID: 1AB4), LpxC of *P. aeruginosa* (PDB ID: 5U39) and *Bacillus anthracis* (PDB ID: 3TYE) were performed using Schrödinger program package [47–49]. The Gaussian 03 suite of programs has been used to locate the structures of the synthesized ligands [50,51]. The ligands 1–10 structures have been located using the Gaussian 03 suite of programs Fig. 2. To perform the calculations the B3LYP model chemistry in combination with the basis sets, 6–31 + G(d,p) for C, H, O, N atoms and 6-311G(d,p) for S atom were used [51–54]. The 2D ligand-receptor interaction diagrams of the desired newly synthesized compounds that have the highest score with the targets and also the 3D binding models of the ligands to the pointed receptors are represented in Figs. 3–6. Also, the 2D ligand-receptor interaction diagrams and the 3D binding models of other ligands to the pointed receptors with the desired bacterial proteins and the Results of interaction diagrams 2D and 3D for Chloramphenicol and Amikacin drugs as positives control can see in the Supporting Information. Besides that the corresponding calculated binding affinity (Glide scores) have been collected in Table 2.

Table 2
Docking scores of the synthesized molecules include bis-tris (imidazoline/thiazolidine)-2,4-dione rings

Ligand	Score			
	Bacillus anthracis (PDB ID: 3TYE)	S. aureus (PDB ID: 3ACX)	E. coli (PDB ID: 1AB4)	P. aeruginosa (PDB ID: 5U39)
1	-5.47	-8.89	-5.13	-7.39
2	-6.20	-7.94	-7.03	-6.88
4a	-5.76	-8.02	-7.90	-5.42
4b	-5.86	-8.84	-7.18	-9.11
5a	-6.55	-9.00	-5.04	-6.38
5b	-5.39	-7.99	-4.89	-6.43
5c	-5.83	-6.73	-5.18	-7.31
7	-6.23	-6.67	-6.80	-9.84
9	-6.59	-8.96	-5.33	-6.11
10	-7.18	-9.05	-6.55	-6.09
Amikacin	-5.82	-6.29	-5.71	-7.70
Chloramphenicol	-4.94	-6.32	-6.23	-5.41

2.2.1. Gyrase A of *E. coli* (PDB ID: 1AB4)

According to the docking results the order of binding energy of the first four molecules appears to be **4a** > **4b** > **2** > **7**, respectively. The type of resulted interactions for structure 4a involve H-bonding between SER-172 and protonated HIS-45 polar groups as hydrogen bond donor and carbonyl groups of one of the five-membered rings, furthermore, there are another H-bonding interaction between ARG-91 as hydrogen bond donor and one of the carbonyl groups of the other five-membered ring, besides that one of the N-H groups of this ring of the ligand act as a hydrogen bond donor to PHE-92 residue while this residue shows a stabilizing π-π stacking interaction with the vicinal benzene ring just bonded to that five-membered ring, thereby providing the greatest binding energy and presumably the most efficient inhibition effect. The presence of internal saturated methylene moiety makes the molecule so flexible to fit well in the active site of the protein to establish the desired interactions. The released energy dominates over the entropy loss of the flexible internal chain. Any structural change such as shortening the length of the internal change (2), increasing the rigidity of this linker (1), or making the terminal groups more sterically hindered would lower the appropriate interactions. Figure 3 shows the optimized structure of compound **4a**, which

has the highest score of interaction with *E.coli* (PDB ID: 1AB4) bacterial proteins, along with 3D and 2D structures.

2.2.2. *S. aureus* (PDB ID: 3ACX)

The noteworthy point is that the calculated scores for this protein are higher than the other three proteins overall. The greatest score obtained for the four highest scores are **10** > **5a** > **1** > **4b**. In the case of **10**, there are two hydrogen bonding interactions, first originated from one N-H group as an H-bond donor toward ASP-114, at the same time the carbonyl group of another five-membered ring behaves as a hydrogen bond acceptor interacting by LYS-273. ARG-171 is simultaneously interacting with two different positions of the ligand, as a hydrogen bond donor to the nitrogen atom of the central S-Triazine ring as well as cation-π with a nearby benzene ring. it seems likely that the presence of rotatable single bonds outward of the S-Triazine ring gives the molecule enough flexibility to adapt the required conformation to fit well in the active site of the protein because the loss of entropy would be compensated by stabilizing interaction between the ligand and surrounding residues benefiting the rule of extension of the structure to establish further interaction. From the 2D interaction diagram, it is understood that just two branches present in structure 10 incorporate interaction with the protein. Comparing the interactions of **10** and **5a** reveals the absence of the hydrogen bond donor effect of ARG-171 toward the nitrogen atom of the central S-Triazine ring of **10** in **5a**, this subtle difference may be invoked to explain the higher binding energy to the extent of 0.05 Kcal mol^{-1} for **10**. Figure 4 shows the optimized structure of compound **10**, which has the highest score of interaction with *S. aureus* (PDB ID: 3ACX) bacterial proteins, along with 3D and 2D structures.

2.2.3. *P. aeruginosa* (PDB ID: 5U39)

In this case, the four highest score structures are **7** > **4b** > **1** > **5c** and there are considerable energy differences between **7** and **4b** with the other structures. In the case of **7**, there is a tendency for both PHE-191 and GLU-198 residues to behave as H-bond acceptors from N-H groups of two terminal five-membered rings. On the other hand, one of the present carbonyl groups accepts H-bond from the protonated Histidine (HIE-19). 2D interaction diagram for **4b** reveals the interactions of two cationic residues, HIP-237 and ARG-201 with carbonyl groups of two different five-membered rings, and ASP-241 takes part in hydrogen bond in combination with one of the N-H groups. Comparing these two structures with others reveals the extent of twisting and bending of the middle part of these molecules to adopt the required conformations to provide the opportunity for observed stabilizing interactions. Figure 5 shows the optimized structure of compound **7**, which has the highest score of interaction with *P. aeruginosa* (PDB ID: 5U39) bacterial proteins, along with 3D and 2D structures.

2.2.4. *B. anthracis* (PDB ID: 3TYE)

The four highest calculated G-score (Glide score) are in the order of **10** > **9** > **5a** > **7**, although **9** and **5a** seem likely to be very close in affinity. The presence of two important binding pocket in this protein have been documented to be pterin and pABA binding pockets. The docking results indicate the occupancy of both mentioned sites by some of the present molecules and establish the stabilizing interactions with relevant residues, for instance, hydrogen bond interaction between one of the oxygen atoms of ether

moiety and the oxygen atom of one of the amide carbonyl groups of molecule **10** with SER-221 and positively charged nitrogen atom of ARG-219 which both of them belong to pABA binding site, while at a distance farther away the amidic N-H group counterparts as H-bond donor toward ASP-149. On the other hand, in the case of molecule **9**, one of the amidic carbonyl groups accepts H-bond from LYN-220 that belongs to the pterin pocket alongside other interactions such as the nearby N-H H-bond with ASP-184, the other vicinal carbonyl group of that ring with amine hydrogen of ASN-120, simultaneous π interaction of attached benzene ring with positively charged ARG-254 and PHE-189 and other interactions that altogether results in the enhanced affinity for that site relative to other remained structures. Figure 6 shows the optimized structure of compound **10**, which has the highest score of interaction with *B. anthracis* (PDB ID: 3TYE) bacterial proteins, along with 3D and 2D structures.

2.3. *Antibacterial activity*

In this investigation, the disk diffusion method tested for the ten newly synthesized molecules with the (bis-tris) imidazolidine/thiazolidine (2,4)-dione biological rings for antibacterial activity. Solutions with a concentration of 0.5 mg/mL were prepared in solvent DMSO and these were tested on the gram-positive bacteria such as Staphylococcus aureus (*S. aureus*) and Bacillus anthracis (*B. anthracis*) and gram-negative bacteria such as Escherichia coli (*E. coli*) and Pseudomonas aeruginosa (*P. aeruginosa*). Chloramphenicol and Amikacin drugs as positive controls were used and they produced significantly sized inhibition zones against the tested bacteria. However, DMSO as negative control did not show observable inhibitory effects against any of the test organisms. These results are shown in Table 3 and Fig. 7.

Table 3
Antibacterial activity of the synthesized molecules by disk diffusion method.

Compounds & Controls	Diameter of growth of inhibition zone (mm)			
	Gram-positive		Gram-negative	
	B. anthracis	S. aureus	E. coli	P. aeruginosa
1	12	27	17	27
2	16	23	24	23
4a	14	25	27	18
4b	16	24	25	31
5a	20	30	17	22
5b	16	22	16	22
5c	17	21	17	25
7	18	20	23	34
9	22	24	18	21
10	24	31	22	20
DMSO(negative control)	-	-	-	-
Amikacin (positive control)	20	21	19	27
Chloramphenicol (positive control)	16	22	21	18
-, no activity				

By reviewing the biological results performed on the Compounds including rings of the (bis-tris) imidazolidine/thiazolidine (2,4)-dione, it seems likely that These compounds appear to exhibit significant antibacterial activity against gram-positive and gram-negative bacteria. Compound **10** with three biological thiazolidine-2,4-dione rings displayed the highest inhibition of bacterial growth against gram-positive *B. anthracis* and *S. aureus* bacteria of 24 mm and 31mm, respectively. Compound **4a**, which has two imidazolidine-2,4-dione rings, indicated a diameter of the inhibitory region of 27mm against gram-negative *E. coli* bacteria. Also, compound **7**, which has two imidazolidine-2,4-dione rings, showed an inhibitory diameter of 34 mm against gram-negative *P. aeruginosa* bacteria. These results are shown in Table 3 and Fig. 7.

2.4. Molecular docking studies for Anticonvulsant Drug Binding (ADB) to the Voltage-Gated Sodium Channel Inner

Pore (VGCIP) (docking protein with synthesized compounds)

Molecular binding of the synthesized compounds, all of which are derivatives of Bis-, and Tris-, imidazolidine/thiazolidine (2,4)-dione, to the active site of the Na-channel, which has a NaVAb voltage-gated, in fact, indicated the possible affinity of the compounds for their biological purpose [55]. In the open structure of the internal pore model, the C-ends of the S6 α-helices of domains I to IV form a wide opening, and some lateral chains face the pore as shown in Figs. 8 and 9. In which all compounds interact stably with amino acid residues. All synthesized molecules exhibit interactions such as polar and H-bonds between the target molecule and the active enzyme of the receptor. The lowest docking score of -10.79 kJ mol^{-1} for combination **10** was observed, which shows the highest combined desire for the channel, while the highest docking score of -5.95 kJ mol^{-1} for combination **4a** was expressed. The results collected in Table 4 reflect their binding affinity as well as the name of the residues that most effectively take part in the interaction with the target molecules.

Table 4
Molecular docking for Anticonvulsant Drug Binding (ADB) to the Voltage-Gated Sodium Channel Inner Pore (VGCIP) of the synthesized molecules

Structure	Score	Interacting groups & Residues
1	-6.44	N-H…O = C (VAL-86), C = O…H-C (LYS-7D), S…H-O (SER-84)
2	-6.53	N-H…O-C (GLU-7B), N-H…O = C (CYS-688), N-H…O = C (ILE-81)
4a	-5.95	N-H…O-H (SER-84), N-H…O = C (ILE-80), N-H…O = C (PHE-87)
4b	-6.84	N-H…O-H (SER-83), N-H…O = C (ASP-7), C = O…H-N (ALA-7C)
5a	-7.53	C = O…H-O (SER-84), N-H…O = C (ILE-80), N-H…O-C (ASP-7)
5b	-6.70	C = O…H-C (THR-87), S…H-C (PHE-91)
5c	-8.31	C = O…H-O (SER-84), N-H…O = C (ILE-80), O (ether)…H-N (ASN-84)
7	-9.23	N-H…O = C (ASN-88), N-H…O = C (ILE-80), C = O…H-O (SER-84)
9	-8.91	C = O…H-O (SER-84), O (ether)…H-O (THR-87), N-H…O = C (VAL-86), N-H…O = C (GLU-7B), C = N…O-H (THR-87)
10	-10.79	N-H…O = C (VAL-86), O (ether)…H-O (THR-87)

For compounds containing two or three Imidazolidine-2,4-dione rings, their binding to the corresponding amino acids at the active site of sodium was investigated. Also, the energy of these compounds is in the range of docking energy according to Table 4 in the range of about − 5.95 to -9.23, which is the most common in compound **4a** and the lowest score common in the **7**. These combinations as seen in Fig. 8,

show several H-bonds interactions with similar amino acids SER-84, GLU-7B, and THR-87 their locations and connecting pattern were nearly the same.

According to Fig. 8, we can see that for combination **7**, the NH group present at the position between two carbonyl groups of IMID-ring established the H-bonding interaction with the carbonyl oxygen of IEL-80 (NH···O = C, 2.3 Å). The carbonyl oxygen of the IMID nucleus formed the H-bonding interaction with SER-84 (C = O···O-H, 2.3 Å) residues. Further, the NH showed the H-bonding interaction with the carbonyl oxygen of ASN-88 (NH···O = C, 2.3 Å).

Compounds containing two and three thiazolidine-2,4-dione rings with amino acids SER-84, THR-87, ILE-80, and VAL-86 have the most interaction in the form of hydrogen bonding.

For these compounds, the docking energy range is about − 6.44 to -10.79, which has combination **1** with the highest score. Also, the product of **10** has three active regions of thiazolidine-2,4-dione and the docking score calculated at -10.79 kJ mol^{-1}according to Table 4 has the lowest docking score among all of the synthesized products. In this product, the NH group between two carbonyls of the TZD nucleus established the H-bonding interaction with the carboxyl oxygen of VAL-86 (NH···O = C, 2.2 Å) residues. Also, the oxygen of ether displayed the H-bond with the OH group of amino acid THR-87 (O···H-O, 1.8 Å) residues, shown in Fig. 9.

According to this docking study Table 4, the four lowest binding docking scores belong to the molecules **5c**, **9**, **7**, and **10** around − 8.31 kJ mol^{-1}, -8.91 kJ mol^{-1}, -9.23 kJ mol^{-1}, and − 10.79 kJ mol^{-1}, respectively and have a good affinity toward the active pocket. Considering structure 7, the presence of the subunits of phenytoin drug would be revealed which in turn may lead to relatively high affinity to the active site. The noteworthy point about all these four compounds is that all of them have been accepted through ADMET evaluation according to the Pfizer rules.

3. Experimental Section

3.1. *Material and Instrument*

The chemical reagents and solvents used in synthesis were purchased from Merck, Fluka, and Sigma-Aldrich. The purity of the synthesized compounds was checked by thin-layer chromatography (TLC) using Merck **silica gel 60F254** aluminum sheets with UV detection. Melting points were determined on the (**91100s**) electric device in open capillary tubes, and are uncorrected. The infrared (IR) spectra were recorded on a (**Shimadzu FT-IR-8400)** spectrometer in the region of 400–4000 cm^{-1}in the KBr disc. A microwave oven (**ETHOS 1600, Milestone**) with a power of 600 W specially designed for organic synthesis was used. ^{1}H NMR and ^{13}C NMR spectra were measured with Bruker 500 and 400 MHz spectrometers in DMSO-d_6 and $CDCl_3$ as solvents. Spectra were internally referenced to Tetramethylsilane

(TMS). All chemical shifts were reported as (ppm) and the coupling constants (J) were reported in hertz. Elemental analysis was made by a (**Carlo-Erba EA1110 CNNO-S**) analyzer and agreed with the calculated values.

3.2. *Preparation of Bis -Tris (thiazolidine/imidazolidine)-2,4-dione*

3.2.1. General method synthesis procedure (bis-tris) thiazolidine-2,4-dione (A):

To a stirred mixture of mono, bis, or tris aldehydes (1.0 mmol) and thiazolidine-2,4-dione (3.0 mmol) in EtOH (25 mL) was added piperidine (0.0064 g, 0.032 mmol) and refluxed at 70–80°C for 24–48 hr. After the completion of the reaction, the reaction mixture was allowed to cool to r. t. and added cold H_2O then acidified with AcOH. The resulting precipitate was filtered and washed successively with H_2O and dried. The precipitate obtained was recrystallized from hot ethanol. The reaction was shown in Scheme 1.

3.2.2. General method synthesis procedure (bis-tris) imidazolidine-2,4-dione (B):

Bis or tris-aldehydes (1.0 mmol) and $(NH_4)_2CO_3$ (4.2 mmol) were dissolved in EtOH 50% (50 mL) and added KCN (2.1 mmol). The solution was stirred and refluxed at 50–70°C for 24–48 hr. After the solution was allowed to cool to r. t., acidified to pH = 2 by the addition of HCl. The precipitated product was filtered, washed with H_2O, dried, and recrystallized from EtOH to give a solid. The reaction was shown in Scheme 1 [41].

3.3. Synthesis of the 1 and 2 compounds

(5Z,5'Z)-5,5'-(1,4-phenylenebis(methaneylylidene))bis(thiazolidine-2,4-dione)– (1)

Following synthesis procedure **method A**, Terephthalaldehyde as a bis-aldehydes reactant and compound **1** was obtained as a Yellow powder as shown in Scheme 1.

Compound **1** (85% yield); m.p: 213–215°C; FT-IR (KBr) ν cm^{-1}: 3133 (N-H stretch); 3038 (aromatic C-H stretching); 1748, 1699 (C = O); 1601 (C = CH stretch); 1158 (C-N stretch); 819, 683 (aromatic C-H out of plane bend). ^{1}H NMR (500 MHz, DMSO-d_6) δ (ppm): 12.73 (s, 2H), 8.02 (s, 2H), 7.81 (s, 4H). ^{13}C NMR (125 MHz, DMSO-d_6) δ (ppm): 167.704, 167.70, 142.26, 138.47, 130.62, 130.41, 130.17, 130.03, and 126.74. HRMS-ESI (*m/z*) [M^+] Calcd. For $C_{14}H_8N_2O_4S_2$ 331.9948, found 330.8978. Elemental Analysis Calcd. For $C_{14}H_8N_2O_4S_2$ (%): C, 50.60; H, 2.43; N, 8.43; O, 19.26; S, 19.29 Found: C, 50.54; H, 2.45; N, 8.47; O, 19.22; S, 19.32.

5,5'-(1,4-Phenylene)bis(imidazolidine-2,4-dione)–(2)

Following synthesis procedure **method B**, terephthalaldehyde as a bis-aldehydes reactant, and compound **2** was obtained as a Cream powder as shown in Scheme 1.

Compound **2** (82% yield); m.p: 295–297°C; FT-IR (KBr) ν cm^{-1}: 3295, 3218 (N-H stretch); 1779, 1714 (C = O); 1192 (C-N stretch); 745, 639 (aromatic C-H out of plane bend). ^{1}H NMR (400 MHz, DMSO-d_6) δ (ppm): 10.92 (s, 2H), 9.03 (s, 2H), 7.45 (s, 4H), 5.28 (s, 2H). ^{13}C NMR (100 MHz, DMSO-d_6) δ (ppm): 174.04, 157.45, 136.05, 126.98, and 60.88. HRMS-ESI (*mlz*) [M^+] Calcd. For $C_{12}H_{10}N_4O_4$ 274.0735, found 274.0024. Elemental Analysis Calcd. For $C_{12}H_{10}N_4O_4$ (%): C, 52.56; H, 3.68; N, 20.43; O, 23.34 Found: C, 52.58; H, 3.62; N, 20.40; O, 23.40.

3.4. *Synthesis of the 4(a-b) and 5(a-c) compounds*

Bis-aldehydes **3(a-c)** used as a precursor were synthesized according to the previously reported procedure [42,56,57].

5,5'-((hexane-1,6-diylbis(oxy))bis(2,1-phenylene))bis(imidazolidine-2,4-dione)– (4a)

Following synthesis procedure **method B**, Product **3a** was a bis-aldehydes reactant, and compound **4a** was obtained as a light yellow powder as shown in Scheme 2 and Table 1.

Compound **4a** (75% yield); m.p: 126–128°C; FT-IR (KBr) ν cm^{-1}: 3363, 3244 (N-H stretch); 3070 (aromatic C-H stretch); 2934, 2861 (aliphatic C-H stretch);1725 (C = O); 1598, 1554, 1496 (aromatic C = C stretch); 1259, 1011 (C-O stretch); 1121 (C-N stretch); 757(aromatic C-H out of plane bending). ^{1}H NMR (400 MHz, DMSO-d_6) δ (ppm): 12.77 (s, 2H), 11.72 (s, 2H), 8.15 (s, 2H), 8.07–8.10 (m, 2H), 7.79–7.83 (m, 2H), 7.57–7.68 (m, 2H), 7.30 (d, J = 2.1 Hz, 2H), 3.13 (t, J = 8.2, 2.3 Hz, 4H), 1.64–1.77 (m, 4H), 1.26–1.37 (m, 4H).^{13}C NMR (100 MHz, DMSO-d_6) δ (ppm): 167.32, 160.78, 156.83, 130.66, 128.20, 122.30, 117.40, 67.96, 43.72, 28.96, and 22.18. HRMS-ESI (*mlz*) [M^+] Calcd. For $C_{24}H_{26}N_4O_6$ 466.1935, found 466.2108. Elemental Analysis Calcd. For $C_{24}H_{26}N_4O_6$ (%): C, 61.79; H, 5.62; N, 12.01; O, 20.58 Found: C, 60.88; H, 5.60; N, 13.40; O, 20.12.

5,5'-((butane-1,4-diylbis(oxy))bis(4,1-phenylene))bis(imidazolidine-2,4-dione)– (4b)

Following synthesis procedure **method B**, Product **3b** was a bis-aldehydes reactant, and compound **4b** was obtained as a light yellow powder as shown in Scheme 2 and Table 1.

Compound **4b** (72% yield); m.p: 180–182°C; FT-IR (KBr) ν cm^{-1}: 3277, 3214 (N-H stretch); 3061 (aromatic C-H stretch); 2926, 2868 (aliphatic C-H stretch);1797, 1717 (C = O); 1598, 1508, 1469 (aromatic C = C stretch); 1246, 1051 (C-O stretch); 1176 (C-N stretch); 745, 638, 602 (aromatic C-H out of plane bending). ^{1}H NMR (400 MHz, DMSO-d_6) δ (ppm): 10.67 (s, 2H), 9.97 (s, 2H), 7.83 (d, J = 4.3 Hz, 4H), 7.07 (d, J = 4.1 Hz, 4H), 5.19 (s, 2H), 4.14 (t, J = 4.2, 2.2 Hz, 4H), 1.96 (t, J = 6.2, 2.0 Hz, 4H).^{13}C NMR (100 MHz, DMSO-d_6) δ (ppm): 174.51, 158.53, 157.40, 131.79, 127.91, 114.55, 67.14, 60.65, and 25.31. HRMS-ESI (mlz) [M^+]

Calcd. For $C_{22}H_{22}N_4O_6$ 438.1545, found 436.8574. Elemental Analysis Calcd. For $C_{22}H_{22}N_4O_6$ (%): C, 60.27; H, 5.06; N, 12.78; O, 21.89 Found: C, 58.88; H, 4.62; N, 15.40; O, 21.10.

(5Z,5'Z)-5,5'-(((hexane-1,6-diylbis(oxy))bis(2,1-phenylene))bis(methaneylylidene))bis(thiazolidine-2,4-dione)– (5a)

Following synthesis procedure **method A**, Product **3a** was a bis-aldehydes reactant, and compound **5a** was obtained as a Yellow powder as shown in Scheme 2 and Table 1.

Compound **5a** (63% yield); m.p: 258–260°C; FT-IR (KBr) v cm^{-1}: 3150 (N-H stretch); 3037 (aromatic C-H stretch); 2941, 2867 (aliphatic C-H stretch); 1740, 1694 (C = O); 1589 (C = CH stretch); 1458, 1453 (aromatic C = C stretch); 1249, 992 (C-O stretch); 1154 (C-N stretch); 751, 686 (aromatic C-H out of plane bending). ^{1}H NMR (500 MHz, DMSO-d_6) δ (ppm): 12.49 (s, 2H), 7.99 (s, 2H), 7.43 (t, J = 6.1, 1.8 Hz, 2H), 7.37 (d, J = 4.6 Hz, 2H), 7.12 (d, J = 4.4 Hz, 2H), 7.06 (t, J = 8.2, 2.4 Hz, 2H), 4.10 (t, J = 6.5, 2.8 Hz, 4H),1.82 (m, 4H), 1.55 (m, 4H).^{13}C NMR (125 MHz, DMSO-d_6) δ (ppm): 167.93, 167.23, 157.52, 132.24, 128.22, 126.23, 121.63, 120.76, 112.77, 68.11, 28.36, and 25.11. HRMS-ESI (mlz) [M^+] Calcd. For $C_{26}H_{24}N_2O_6S_2$ 524.1133, found 523.6512. Elemental Analysis Calcd. For $C_{26}H_{24}N_2O_6S_2$ (%): C, 59.53; H, 4.61; N, 5.34; O, 18.30; S, 12.22 Found: C, 57.35; H, 5.42; N, 6.40; O, 20.11; S, 10.72.

(5Z,5'E)-5,5'-(((butane-1,4-diylbis(oxy))bis(4,1-phenylene))bis(methaneylylidene))bis(thiazolidine-2,4-dione)– (5b)

Following synthesis procedure **method A**, Product **3b** as a bis-aldehydes reactant, and the compound **5b** was obtained as a white powder as shown in Scheme 2 and Table 1.

Compound **5b** (77% yield); m.p: 166–168°C; FT-IR (KBr) v cm^{-1}: 3235 (N-H stretch); 3132 (aromatic C-H stretch); 2950, 2878 (aliphatic C-H stretch);1738, 1695 (C = O); 1602(C = CH stretch); 1573, 1511 (aromatic C = C stretch); 1256 (C-O stretch); 1158 (C-N stretch); 831, 651 (aromatic C-H out of plane bending). ^{1}H NMR (500 MHz, DMSO-d_6) δ (ppm): 12.49 (s, 2H), 7.85 (d, J = 6.6 Hz, 4H), 7.74 (s, 2H), 7.11 (t, J = 8.4, 2.6 Hz, 4H), 4.14 (t, J = 8.2, 2.4 Hz, 4H), 1.91 (t, J = 7.6, 2.8 Hz, 4H). ^{13}C NMR (125 MHz, DMSO-d_6) δ (ppm): 167.87, 167.37, 160.34, 131.75, 129.57, 115.35, 114.90, 67.66, and 25.12. HRMS-ESI (mlz) [M^+] Calcd. For $C_{24}H_{20}N_2O_6S_2$ 496.0844, found 494.6231. Elemental Analysis Calcd. For $C_{24}H_{20}N_2O_6S_2$ (%): C, 58.05; H, 4.06; N, 5.64; O, 19.33; S, 12.91 Found: C, 59.77; H, 3.68; N, 6.40; O, 18.21; S, 11.94.

(5Z,5'Z)-5,5'-((((1,4-phenylenebis(methylene))bis(oxy))bis(4,1-phenylene))bis(methaneylylidene))bis(thiazolidine-2,4-dione)– (5c)

Following synthesis procedure **method A**, Product **3c** was a bis-aldehydes reactant, and the compound **5c** was obtained as a light yellow powder as shown in Scheme 2 and Table 1.

Compound **5c** (78% yield); m.p: 216–218°C; FT-IR (KBr) ν cm^{-1}: 3107 (N-H stretch); 2959 (aromatic C-H stretch); 2931, 2872 (aliphatic C-H stretch); 1731, 1689 (C = O); 1600 (C = CH stretch); 1510, 1463, 1424 (aromatic C = C stretch); 1251, 1001 (C-O stretch); 1158 (C-N stretch); 886,831, 797 (aromatic C-H out of plane bending). ^{1}H NMR (500 MHz, DMSO-d_6) δ (ppm): 11.61 (s, 2H), 9.03 (s, 2H), 7.04–7.05 (m, 2H), 6.72 (d, *J* = 6.3 Hz, 2H), 6.66 (d, *J* = 1.4 Hz, 4H), 6.37 (d, *J* = 7.2, 4H), 4.41 (s, 4H).^{13}C NMR (125 MHz, DMSO-d_6) δ (ppm): 163.25, 162.26, 136.23, 132.03, 131.80, 129.85, 128.00, 127.96, 125.83,115.75,115.33, and 69.41. HRMS-ESI (mlz) [M^+] Calcd. For $C_{28}H_{20}N_2O_6S_2$ 544.0824, found 545.1452. Elemental Analysis Calcd. For $C_{28}H_{20}N_2O_6S_2$ (%): C, 61.75; H, 3.70; N, 5.14; O, 17.63; S, 11.77 Found: C, 63.36; H, 4.82; N, 4.40; O, 15.85; S, 11.57.

3.5. Synthesis of the 6 compound

5-(4-hydroxyphenyl)-5-phenylimidazolidine-2,4-dione –(6)

Following synthesis procedure **method B**, 4-hydroxy benzophenone as an aldehyde reactant and compound **6** was obtained as a light yellow powder as shown in Scheme 3.

Compound **6** (61% yield); m.p: 182–185°C; FT-IR (KBr) ν cm^{-1}: 3265, 3147 (N-H stretch); >3000 broad peaks (O-H stretch); 1725, 1630 (C = O); 1601, 1562, 1512 (aromatic C = C stretch); 1238, 1035 (C-O stretch); 1146 (C-N stretch); 841, 741, 695 (aromatic C-H out of plane bending). ^{1}H NMR (500 MHz, DMSO-d_6) δ (ppm): 11.00 (s, 1H), 10.45 (s, 1H), 9.17 (s, 1H), 7.31–7.40 (m, 5H), 7.11 (d, *J* = 8.3 Hz, 2H), 6.75 (d, *J* = 8.2 Hz, 2H). ^{13}C NMR (125 MHz, DMSO-d_6) δ (ppm): 175.68, 162.42, 157.53, 138.54, 132.96, 129.57, 128.82, 127.03, 115.70, and 70.30. HRMS-ESI (*mlz*) [M^+] Calcd. For $C_{15}H_{12}N_2O_3$ 268.0854, found 269.1684. Elemental Analysis Calcd. For $C_{15}H_{12}N_2O_3$ (%): C, 67.16; H, 4.51; N, 10.44; O, 17.89 Found: C, 70.10; H, 5.32; N, 12.41; O, 12.17.

5,5'-(((1,4-phenylenebis(methylene))bis(oxy))bis(4,1-phenylene))bis(5-phenylimidazolidine-2,4-dione)– (7)

To a mixture of Product **6** (2.0 mmol), 1,4-bis(chloromethyl)benzene (1.0 mmol) in DMF (10 mL) was added K_2CO_3 (1.0 mmol, 0.11g), was refluxed for 24 hr. then the reaction mixture was placed in an ice-water bath and H_2O was added to it. After it was stirred for 30 min and the precipitates of the product were filtered, washed with H_2O, and recrystallized with EtOH, Compound **7** was obtained as a light pink powder as shown in Scheme 3.

Compound **7** (47% yield); m.p: 167–170°C; FT-IR (KBr) ν cm^{-1}: 3281 (N-H stretch); 3058 (aromatic C-H stretch); 2930, 2889 (aliphatic C-H stretch); 1773, 1713 (C = O); 1643, 1598 (aromatic C = C stretch); 1248, 1003 (C-O stretch); 1174 (C-N stretch); 842, 698 (aromatic C-H out of plane bending). ^{1}H NMR (400 MHz, DMSO-d_6) δ (ppm): 11.01 (s, 2H), 10.66 (s, 2H), 7.81–7.89 (m, 2H), 7.81 (t, *J* = 8.4, 2.3 Hz, 3H), 7.66–7.70 (m, 3H), 7.55 (d, *J* = 7.9 Hz, 1H), 7.47 (dd, *J* = 8.3 Hz, 4H), 7.38 (d, *J* = 8.1 Hz, 1H), 7.21–7.32 (m, 4H), 6.88 (d, *J* = 8.4 Hz, 4H), 5.31 (s, 4H). ^{13}C NMR (100 MHz, DMSO-d_6) δ (ppm): 173.38, 157.12, 155.06, 132.14,

129.23, 128.43, 128.11, 127.99, 127.85, 127.40, 126.54, 115.17, 75.89, and 69.22. HRMS-ESI (*m/z*) [M^+] Calcd. For $C_{38}H_{30}N_4O_6$ 638.2236, found 636.5438. Elemental Analysis Calcd. For $C_{38}H_{30}N_4O_6$ (%): C, 71.46; H, 4.73; N, 8.77; O, 15.03 Found: C, 69.98; H, 5.74; N, 7.65; O, 16.63.

3.6. Synthesis of the 9 and 10 compounds

4,4',4"-((1,3,5-Triazine-2,4,6-triyl)tris(oxy))tribenzaldehyde– (8)

A mixture of *p*-hydroxybenzaldehyde (6 mmol, 0.733 g), NaOH (8 mmol, 0.32g), and H_2O (20 mL) was added to the suspension of cyanuric chloride (2 mmol, 0.36 g) in dry acetone (50 mL) at 0–5°C and this was stirred for 5 hr. After that, the solid was collected by filtration and washed three times with H_2O. Then, the product was isolated by recrystallization from EtOAc. Product **8** was prepared as white powder as shown in Scheme 4.

Compound **8** (90% yield); m.p: 180–181°C; FT-IR (KBr) ν cm^{-1}: 3068 (aromatic C-H stretch); 1702 (C = O); 1568 (C = N stretch); 1367, 1212 (C-O stretch); 1160 (C-N stretch); 838 (aromatic C-H out of plane bending). ^{1}H NMR (500 MHz, DMSO-d_6) δ (ppm): 9.98 (*s*, 1H), 7.97 (*d*, *J* = 8.2 Hz, 2H), 7.48 (*d*, *J* = 8.2 Hz, 2H). ^{13}C NMR (125 MHz, DMSO-d_6) δ (ppm): 191.82, 172.68, 155.60, 134.06, 131.10, and 122.29. HRMS-ESI (*m/z*) [M^+] calcd. For $C_{24}H_{15}N_3O_6$ 441.0961, found 441.0967. Elemental Analysis Calcd. For $C_{24}H_{15}N_3O_6$ (%): C, 65.31; H, 3.43; N, 9.52; O, 21.75 Found: C, 66.12; H, 3.45; N, 8.47; O, 21.96.

5,5',5"-(((1,3,5-triazine-2,4,6-triyl)tris(oxy))tris(benzene-4,1-diyl))tris(imidazolidine-2,4-dione)– Tripod (9)

Following synthesis procedure **method B**, Product **8** was a tris-aldehyde reactant and compound **9** was obtained as a cream powder as shown in Scheme 4.

Compound **9** (65% yield); m.p: 268–270°C; FT-IR (KBr) ν cm^{-1}: 3327, 3193 (N-H stretch); 1733, 1671 (C = O); 1617, 1510, 1455 (aromatic C = C stretch); 1252, 1090 (C-O stretch); 1190 (C-N stretch); 784, 640 (aromatic C-H out of plane bending). ^{1}H NMR (400 MHz, DMSO-d_6) δ (ppm): 11.19 (s, 1H), 10.71 (s, 1H), 7.51–7.54 (m, 2H), 7.16–7.21 (m, 2H), 6.12 (s, 1H). ^{13}C NMR (100 MHz, DMSO-d_6) δ (ppm): 182.68, 173.60, 157.82, 150.40, 134.19, 131.33, 127.78, and 70.09. HRMS-ESI (*m/z*) [M^+] Calcd. For $C_{30}H_{21}N_9O_9$ 651.1568, found 650.9984. Elemental Analysis Calcd. For $C_{30}H_{21}N_9O_9$ (%): C, 55.30; H, 3.25; N, 19.35; O, 22.10 Found: C, 53.54; H, 3.45; N, 18.97; O, 24.04.

(5,5',5"-((((1,3,5-Triazine-2,4,6triyl)tris(oxy))tris(benzene-4,1-diyl))tris(methaneylylidene))tris (thiazolidine-2,4-dione)) – Tripod (10)

Following synthesis procedure **method A**, Product **8** was a tris-aldehyde reactant, and tripod **10** was obtained as a yellow powder as shown in Scheme 4.

Tripod **10** (87% yield); m.p: 244–246°C; FT-IR (KBr) ν cm^{-1}: 3131 (N-H stretch); 3008 (aromatic C-H stretch); 1755, 1691 (C = O); 1589 (C = CH stretch); 1504, 1377, 1338 (aromatic C = C stretch); 1216, 1009

(C-O stretch); 1152 (C-N stretch); 824,690 (aromatic C-H out of plane bending). ^{1}H NMR (500 MHz, DMSO-d_6) δ (ppm): 12.44 (s, 1H), 7.69 (s, 1H), 7.44 (d, J = 8.5 Hz, 2H), 6.90 (d, J = 8.5, 2H).^{13}C NMR (125 MHz, DMSO-d_6) δ (ppm): 171.27, 167.68, 167.44, 159.87, 152.93, 132.34, 131.17, 122.43, and 116.30. HRMS-ESI (*m/z*) [M^+] calcd. For $C_{33}H_{18}N_6O_9S_3$ 738.0297, found 738.0308. Elemental Analysis Calcd. For $C_{33}H_{18}N_6O_9S_3$ (%): C, 53.66; H, 2.46; N, 11.38; O, 19.49; S, 13.02 Found: C, 52.58; H, 2.62; N, 11.40; O, 20.10; S, 13.30.

3.7. Antimicrobial activities by Inhibition zone diameter assay

Using a slightly disk diffusion method (DDM), the antibacterial activity of ten newly synthesized molecules was determined. The disk diffusion method is among the most flexible susceptibility testing methods in terms of antimicrobial agents that can be tested. The method consists of placing paper disks saturated with antimicrobial agents on a lawn of bacteria seeded on the surface of an agar medium, incubating the plate overnight, and measuring the presence or absence of a zone of inhibition around the disks [58]. Muller Hinton agar was used for the growth of bacterial strains such as gram-positive Staphylococcus aureus *(S. aureus)* and Bacillus anthacis *(B. anthracis)* bacteria and gram-negative Escherichia coli *(E. coli)* and Pseudomonas aeruginosa *(P. aeruginosa)* bacteria. All of the test compounds were dissolved in DMSO at a conc. of 0.5 mg/ml. Each plate was inoculated with 20 µl of microbial suspension. 30 µl of the test compounds were added to each disk. The plates containing bacteria were incubated at 37 ^{o}C for 24 h., the positive antimicrobial activity was read based on the growth inhibition zone, and compared with Chloramphenicol and Amikacin were used as a positive control and DMSO as a negative control [58–60], as shown in Table 3 and Fig. 7.

4. Conclusions

This study was performed to predict the prospects of new compounds including (bis-tris) imidazolidine/thiazolidine (2,4)-dione rings, docking simulation studies were performed to investigate them as anticonvulsants and also as antibacterial agents. These derivatives were synthesized using the optimization two and three directional 3 and 4MCR Knoevenagel condensation (**method A**) and two and three directional 5 and 7 MCR Bucherer-Bergs (**method B**). Since phenytoin is used as a common anticonvulsant drug and has a high affinity for binding to the Na^+ channel, and with the non-polar side chains of the S6 helix, it shows amplitudes I to IV, accordingly, this drug was used as a competitive benchmark for the compounds synthesized as anticonvulsants. The results showed that all of these compounds experienced high polarity levels due to their biologically active imidazolidine and thiazolidine (2,4)- dione rings, which have atoms with high electronegative levels.

The high polarity of the synthesized compounds results in abundant and varied H-bonds with amino acids at active sites. The two amino acids SER-84 and ILE-80 had the highest bond interaction with synthetic compounds, and among them, **10** and **7** showed the lowest simulation score. Composition **10**

has − 10.79 KJ mol-1 the binding energy is lowly regarded due to the presence of three active groups of thiazolidine-2,4-dione. Combination **7** has − 9.23 KJ mol-1 as the docking score, showing interesting results due to having two phenytoin drugs that were connected by a linker. On the other hand, according to the docking Antibacterial results, compound **10** has a binding affinity with gram-positive *Bacillus anthracis* (PDB ID: 3TYE) at around − 7.18 kcal/mol and − 9.05 kcal/mol with *S. aureus* (PDB ID: 3ACX). This compound has the highest scores among all compounds against gram-positive bacteria. For *E. coli* (PDB ID: 1AB4) gram-negative bacteria, compound **4a** displays a high score of almost − 7.90 among other compounds. Also, the highest binding affinity is related to compound **7**, about − 9.84 for gram-negative *P. aeruginosa* (PDB ID: 5U39) bacterial proteins.

Meanwhile, experimental results of bacterial tests show that the highest diameter of inhibition of growth zone against gram-positive bacteria *(B. anthracis) and (S. aureus)* belongs to the combination containing three thiazolidine-2,4-dione rings (compound **10**) about 24 mm and 31 mm, respectively. Also, the combinations containing two imidazole-2,4-dione rings against gram-negative bacteria have a higher diameter of growth zone inhibition, compounds **4a** and **7** for *(E. coli)* and *(P. aeruginosa)* bacteria almost 27 mm and 34 mm, respectively.

Declarations

Acknowledgments

This probe was supported in part by the Research Committee of the University of Guilan.

Ethical Approval

Not applicable

Competing interests

No competing interests

Authors' contributions

N. O. Mahmoodi, supervised the findings of this work, conceived the presented idea and edited.

H. Yazdani Nyaki, conceived the presented idea, developed the theory, synthesized all compounds and prepared and revised figures and Tables, and fit them into the Manuscript.

H. Taherpour Nahzomi, performed the computations of a Molecular Docking Study for Antibacterial Effect and Molecular docking studies for Anticonvulsant Drug Binding (ADB) to the Voltage-Gated Sodium Channel Inner Pore (VGCIP) (docking protein with synthesized compounds).

E. Panahi Kokhdan, performed the Antibacterial test and verified the analytical methods.

All authors discussed the results and contributed to the final manuscript.

Funding

The Research Committee of the University of Guilan

Availability of data and materials

The data that support the findings of this study are openly available in within the article [and/or] its supplementary materials.

References

1. N. C. Desai, U. P. Pandit, and A. Dodiya, Expert Opin. Ther. Pat. **25**, 479 (2015).
2. S. Kaur Manjal, R. Kaur, R. Bhatia, K. Kumar, V. Singh, R. Shankar, R. Kaur, and R. K. Rawal, Bioorg. Chem. **75**, 406 (2017).
3. L. Konnert, J. Martinez, E. Colacino, M. Enscm, Recent Advances in the Synthesis of Hydantoins : The State of the Art of a Valuable Scaffold (2017).
4. L. Konnert, B. Reneaud, R. M. De Figueiredo, J. M. Campagne, F. Lamaty, J. Martinez, and E. Colacino, J. Org. Chem. **79**, 10132 (2014).
5. V. Asati, D. K. Mahapatra, and S. K. Bharti, Eur. J. Med. Chem. **87**, 814 (2014).
6. A. M. Youssef, M. Sydney White, E. B. Villanueva, I. M. El-Ashmawy, and A. Klegeris, Bioorganic Med. Chem. **18**, 2019 (2010).
7. F. Ghanbari Pirbasti, N. O. Mahmoodi, and J. Abbasi Shiran, J. Sulfur Chem. **37**, 196 (2016).
8. A. A. Elhenawy, A. A. A. Salama, M. M. A. All, A. A. Alomri, and H. S. Nassar, Int. J. Pharm. Sci. Rev. Res. **31**, 23 (2015).
9. A. I. Khodair and P. Bertrand, Tetrahedron **54**, 4859 (1998); b) N.O..Mahmoodi, Z. Khodaee, Arkivoc. **3,** 29 (2007).
10. B. F. Abdel-Wahab, G. E. A. Awad, and F. A. Badria, Eur. J. Med. Chem. **46**, 1505 (2011); b) N.O. Mahmoodi, Z. Khodaee, Mendeleev Commun. **14**, 304 (2004).
11. 11. M. C. Kandemir, A. Saları, B. Bıçak, and S. K. Gündüz, 3 (2019); b) Z. Khodaeea, N.O. Mahmoodi, A. Yahyazadeh, Org. Chem. Res., **3** (2), 112 (2017).
12. H. Kumar, A. Deep, and R. K. Marwaha, BMC Chem. **14**, 1 (2020).
13. M. S. Hill, D. J. Liptrot, and M. F. Mahon, Angew. Chemie - Int. Ed. **52**, 5364 (2013).
14. L. Vatannavaz, S. J. Sabounchei, A. Sedghi, R. Karamian, S. H. M. Farida, and N. Rahmani, Polyhedron **181**, 114478 (2020).
15. Y. nan Sun, Z. xuan Yang, F. zheng Ren, and B. Fang, Int. J. Biol. Macromol. **158**, 401 (2020).
16. H. Gao, L. Ding, R. Liu, X. Zheng, X. Xia, F. Wang, J. Qi, W. Tong, and Y. Qiu, Int. J. Biol. Macromol. **179**, 259 (2021).

17. K. Dhara, S. Paladhi, G. C. Midya, and J. Dash, Org. Biomol. Chem. **9**, 3801 (2011).
18. N. Chadha, M. S. Bahia, M. Kaur, and O. Silakari, Bioorganic Med. Chem. **23**, 2953 (2015).
19. N. Kumar, S. Thomas, R. Rao, N. Maiti, and R. J. Kshirsagar, J. Phys. Chem. A **123**, 9770 (2019).
20. Y. C. Chen, S. Da Huang, J. H. Tu, J. S. Yu, A. O. Nurlatifah, W. C. Chiu, Y. H. Su, H. L. Chang, D. A. Putri, and H. L. Cheng, Int. J. Biol. Macromol. **146**, 202 (2020).
21. N. Dieltiens, D. D. Claeys, and C. V. Stevens, J. Org. Chem. **71**, 3863 (2006).
22. V. Haridas, S. Sadanandan, G. Hundal, and C. H. Suresh, Tetrahedron Lett. **53**, 5523 (2012).
23. B. Hosseinzadeh, A. S. Beni, M. Azari, M. Zarandi, and M. Karami, New J. Chem. **40**, 8371 (2016).
24. N. Sepay, S. Mallik, P. C. Saha, and A. K. Mallik, New J. Chem. **42**, 15270 (2018).
25. Y. Wang, P. J. Jones, T. W. Batts, V. Landry, M. K. Patel, and M. L. Brown, Bioorganic Med. Chem. **17**, 7064 (2009).
26. Y. Yaari, M. E. Selzer, and G. David, Brain Res. **345**, 102 (1985).
27. S. Botros, N. A. Khalil, B. H. Naguib, and Y. El-Dash, Eur. J. Med. Chem. **60**, 57 (2013).
28. M. Sitges, L. M. Chiu, and R. C. Reed, Neurochem. Res. **41**, 758 (2016).
29. D. Ali, S. Alarifi, S. Kumar, S. Kumar, and I. Akbar, J. Infect. Public Health **13**, 1951 (2020).
30. a) Y. Ma, T.T. Ding, Y.Y. Liu, Z.H. Zheng, S.X. Sun, L.S. Zhang, H. Zhang, X.H. Lu, X.C. Cheng, R.L. Wang. Biochem Biophys Res Commun. **19**, 40 (2021); b) L. Zare, N.O. Mahmoodi, A. Yahyazadeh, M. Mamaghani, Synthet. Communi. 41 (15) 2323 (2011); c) L. Zare, N.O. Mahmoodi, A. Yahyazadeh, M. Mamaghani, J. Heterocycl. Chem. **48**, 864 (2011).Khalil Tabatabaeian.
31. A. Keivanloo, S. Lashkari, S. Sepehri, M. Bakherad, and S. Abbaspour, Monatshefte Für Chemie - Chem. Mon. **6,** 151 (2020).
32. N.O. Mahmoodi, S. Emadi, One-Pot Synthesis of Phenytoin Analogs. Russian Journal of Organic Chemistry **40**, 377 (2004).
33. N. Trotsko, J. Golus, P. Kazimierczak, A. Paneth, A. Przekora, G. Ginalska, and M. Wujec, Bioorg. Chem. **97**, 103676 (2020).
34. S. G. Alegaon and K. R. Alagawadi, Med. Chem. Res. **21**, 816 (2012).
35. A. Keivanloo, S. Lashkari, S. Sepehri, M. Bakherad, and S. Abbaspour, J. Chinese Chem. Soc. **68**, 1317 (2021).
36. M. Y. Yu, S. N. Liu, H. Liu, Q. H. Meng, X. J. Qin, and H. Y. Liu, Bioorg. Chem. **117**, 105404 (2021).
37. H. R. Umesh, K. V. Ramesh, and K. S. Devaraju, Beni-Suef Univ. J. Basic Appl. Sci. **9**, (2020).
38. V. R. Avupati, R. P. Yejella, A. Akula, G. S. Guntuku, B. R. Doddi, V. R. Vutla, S. R. Anagani, L. S. Adimulam, and A. K. Vyricharla, Bioorganic Med. Chem. Lett. **22**, 6442 (2012).
39. M. R. Ganjali, F. Faridbod, R. Dinarvand, P. Norouzi, and S. Riahi, Sensors **8**, 1645 (2008).
40. A. L. Doadrio, J. M. Sánchez-Montero, J. C. Doadrio, A. J. Salinas, and M. Vallet-Regí, Microporous Mesoporous Mater. **195**, 43 (2014).
41. Z. Khodaee, A. Yahyazadeh, and N. O. Mahmoodi, J. Heterocycl. Chem. **50**, 288 (2013).

42. N. O. Mahmoodi, J. Parvizi, B. Sharifzadeh, and M. Rassa, Arch. Pharm. (Weinheim). **346**, 860 (2013).
43. J. Riedner and P. Vogel, Tetrahedron Asymmetry **15**, 2657 (2004).
44. M. M. Zeydi and O. Mahmoodi, Int. J. Recent Adv. Multidiscip. Res. **3**, 2052 (2016).
45. a) N. O. Mahmoodi and M. M. Zeydi, J. Iran. Chem. Soc. **15**, 311 (2018); b) N. O. Mahmoodi, K. Tabatabaeian, H Kiyani, Helv. Chim. Acta, **95** (3), 536 (2012).
46. H. Yazdani Nyaki, N. O. Mahmoodi, M. Pasandideh Nadamani, Can. J. Chem. **99**, 482 (2021).
47. a) J. Román, A. Castillo, and A. Mahn, Molecules **23**, 1313 (2018); b) K. Rad-Moghadam, N. O. Mahmoodi, F. Asghari-Haji, RSC Advance, **6** (33) 27388 (2016)
48. S. Triloknadh, C. Venkata Rao, K. Nagaraju, N. Hari Krishna, C. Venkata Ramaiah, W. Rajendra, D. Trinath, and Y. Suneetha, Bioorganic Med. Chem. Lett. **28**, 1663 (2018).
49. G. Palareti, C. Legnani, B. Cosmi, E. Antonucci, N. Erba, D. Poli, S. Testa, and A. Tosetto, Int. J. Lab. Hematol. **38**, 42 (2016).
50. a) S. F. Boys and F. Bernardi, Mol. Phys. **19**, 553 (1970); b) N. O. Mahmoodi and S. Ghodsi, Res. Chem. Intermed. 43, 661 (2017).
51. a) R. F. W. Bader, Acc. Chem. Res. **18**, 9 (1985); b) A. Sheykhi-Estalkhjani, N. O. Mahmoodi, A. Yahyazadeh, and M. Pasandideh Nadamani, Res. Chem. Intermed. **46**, 3835 (2020).
52. A. D. Becke, J. Chem. Phys. **98**, 5648 (1993).
53. C. Lee, W. Yang, and R. G. Parr, Phys. Rev. B **37**, 785 (1988).
54. S. H. Vosko, L. Wilk, and M. Nusair, Can. J. Phys. **58**, 1200 (1980).
55. D. K. Mahapatra, D. Das, R. S. Shivhare, and S. S. Borkar, MOJ Bioorganic Org. Chem. **2**, 46 (2018).
56. J. Klenc, E. Raux, S. Barnes, S. Sullivan, B. Duszynska, A. J. Bojarski, and L. Strekowski, J. Heterocycl. Chem. **46**, 1259 (2009).
57. J. Parvizi, N. O. Mahmoodi, F. G. Pirbasti, and M. Rassa, ChemistrySelect **4**, 5421 (2019).
58. a) F. C. Tenover, Encycl. Microbiol. 166 (2019); b) N.O. Mahmoodi, F. Ghanbari Pirbasti, Z. Jalalifard, J. Chin. Chem. Soc. **65** (4) 383 (2018)
59. H. Y. Nyaki and N. O. Mahmoodi, Res. Chem. Intermed. **47**, 4129 (2021); b) N. O. Mahmoodi, B. Khalili, O. Rezaeianzade, and A. Ghavidast, Res. Chem. Intermed. **42**, 6531 (2016).
60. L. Zare, N.O. Mahmoodi, A. Yahyazadeh, M. Mamaghani, K. Tabatabaeian Chin. Chem. Lett. **21** (5), 538 (2010).

Schemes

Schemes 1 to 4 are available in the Supplementary Files section.

Figures

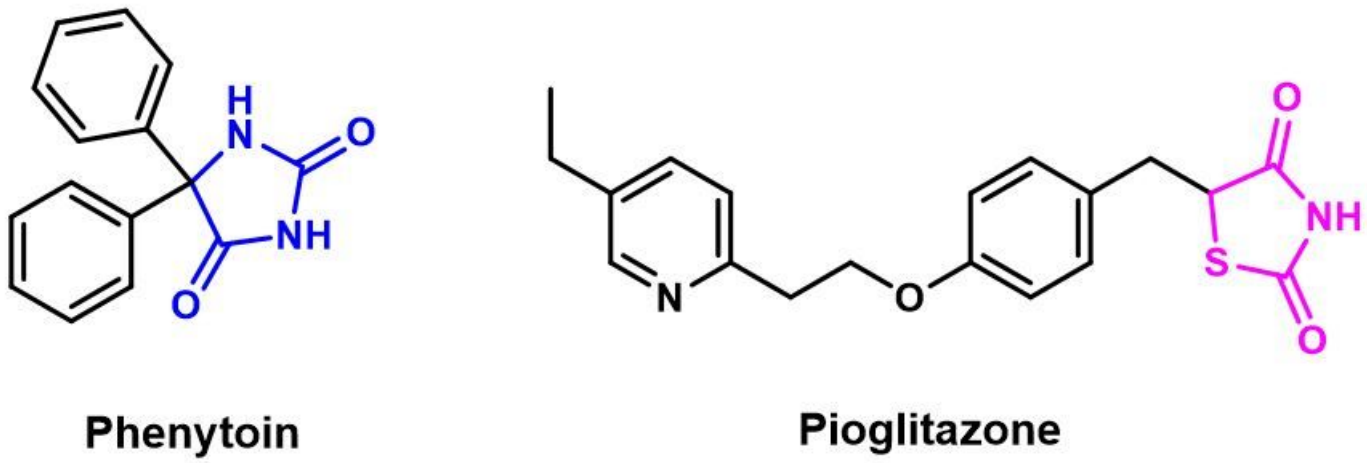

Figure 1

Clinical drugs including imidazoline-2,4-dione (Phenytoin) and thiazolidine-2,4-dione (Pioglitazone) rings.

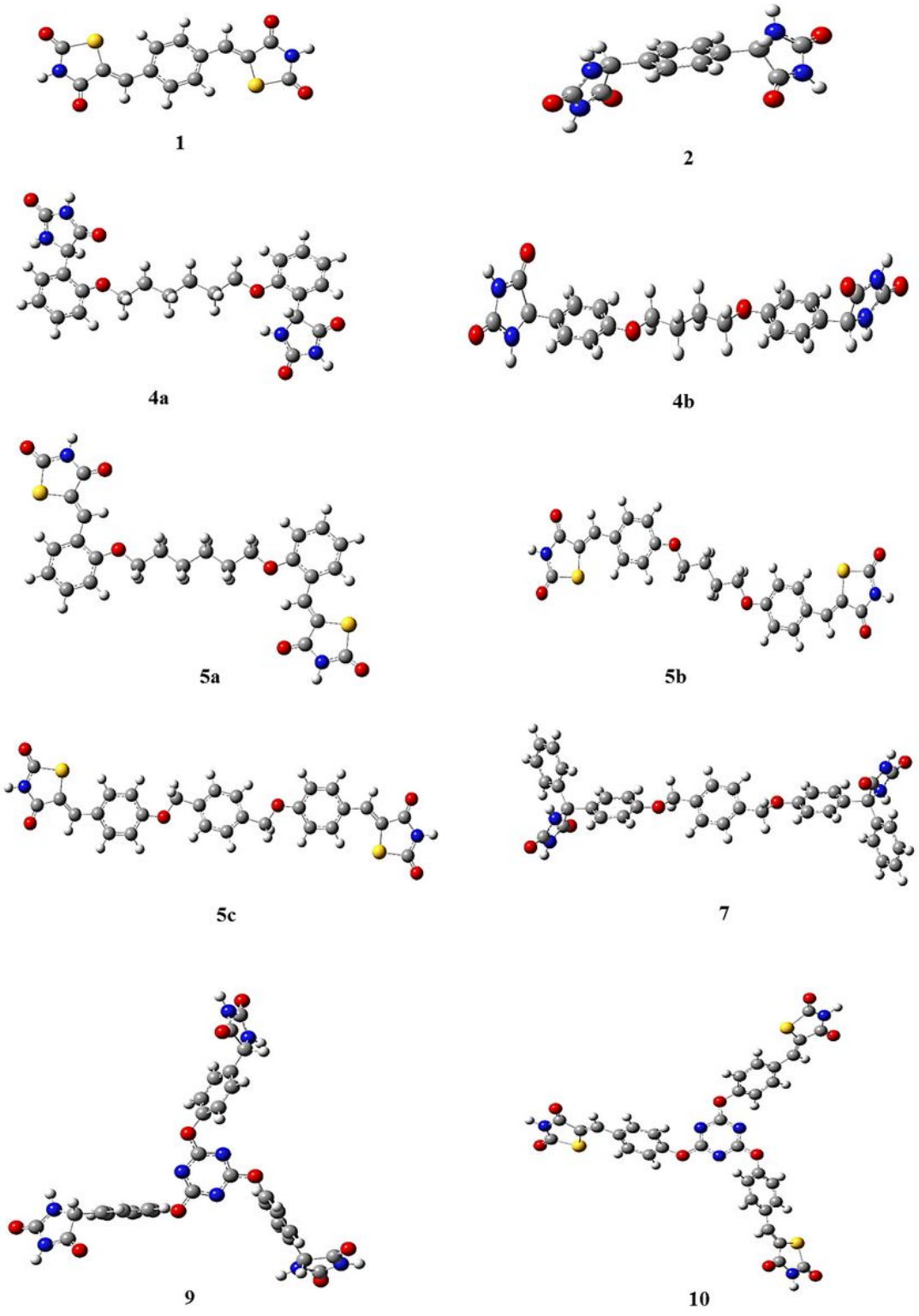

Figure 2

The optimized structures were obtained at the B3LYP/6–31 + G (d,p)/ 6–311 + G(d,p) level of theory

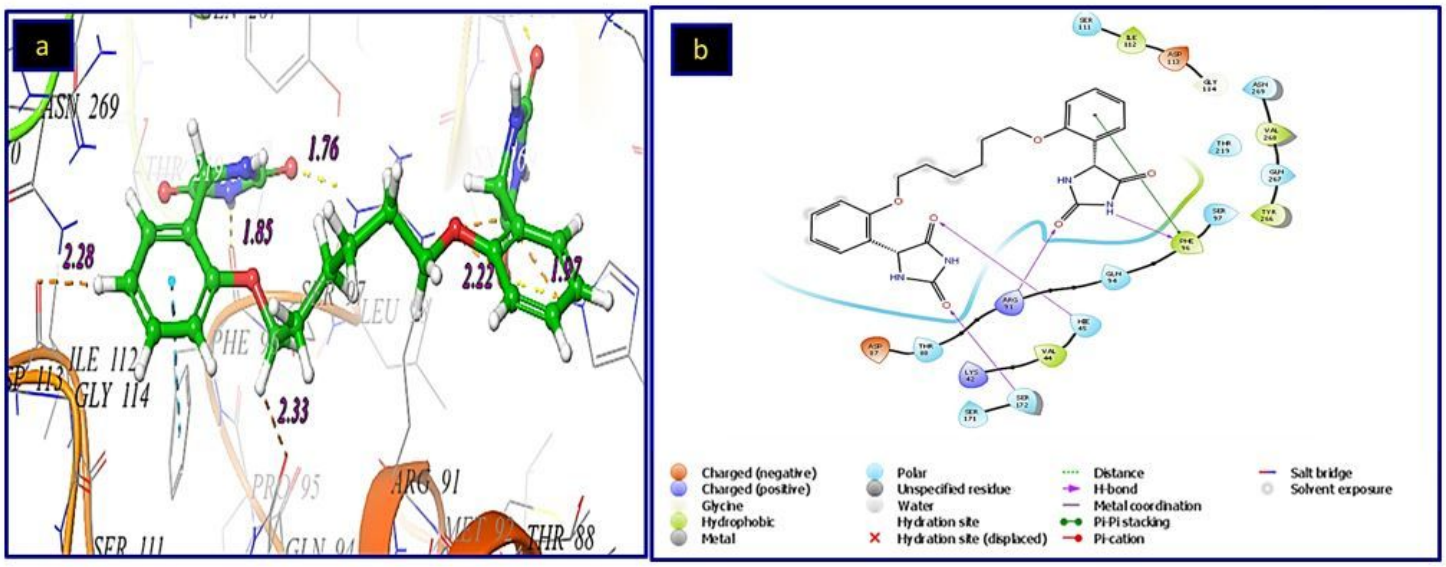

Figure 3

a) The binding mode of the **4a** ligand with the binding site of Gyrase A of *E. coli*(PDB Id: 1AB4) and **b)** 2D ligand-receptor interaction with 1AB4 enzyme.

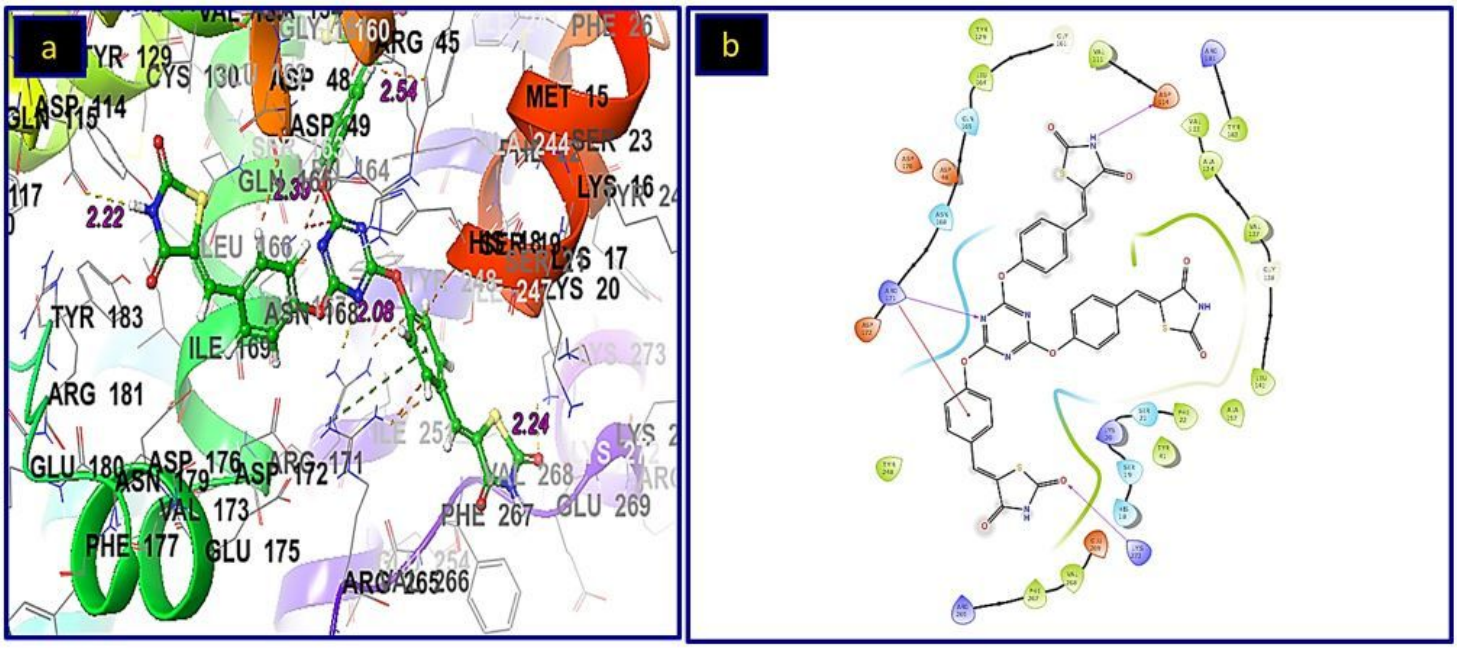

Figure 4

a) The binding mode of **10** ligand with *S. aureus* (PDB Id: 3ACX)and **b)** 2D ligand-receptor interaction with 3ACX enzyme.

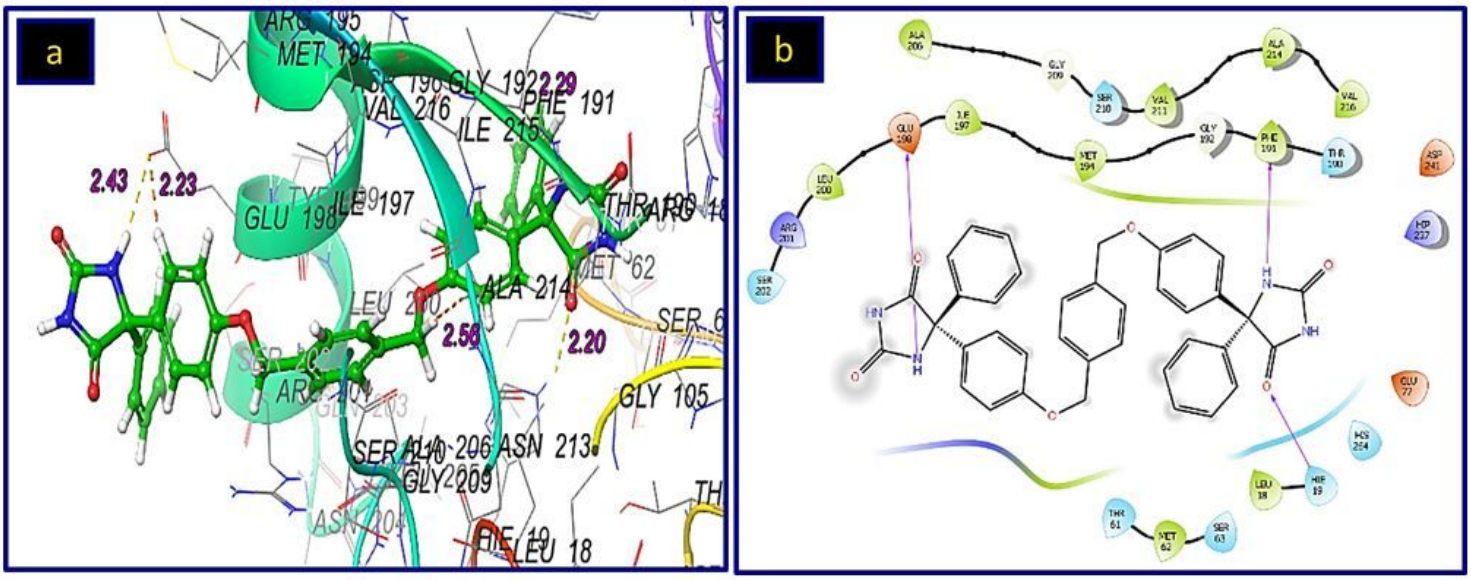

Figure 5

a) The binding mode of **7** ligand with LpxC of *P. aeruginosa* (PDB Id: 5U39) and **b)** 2D ligand-receptor interaction with 5U39 enzyme.

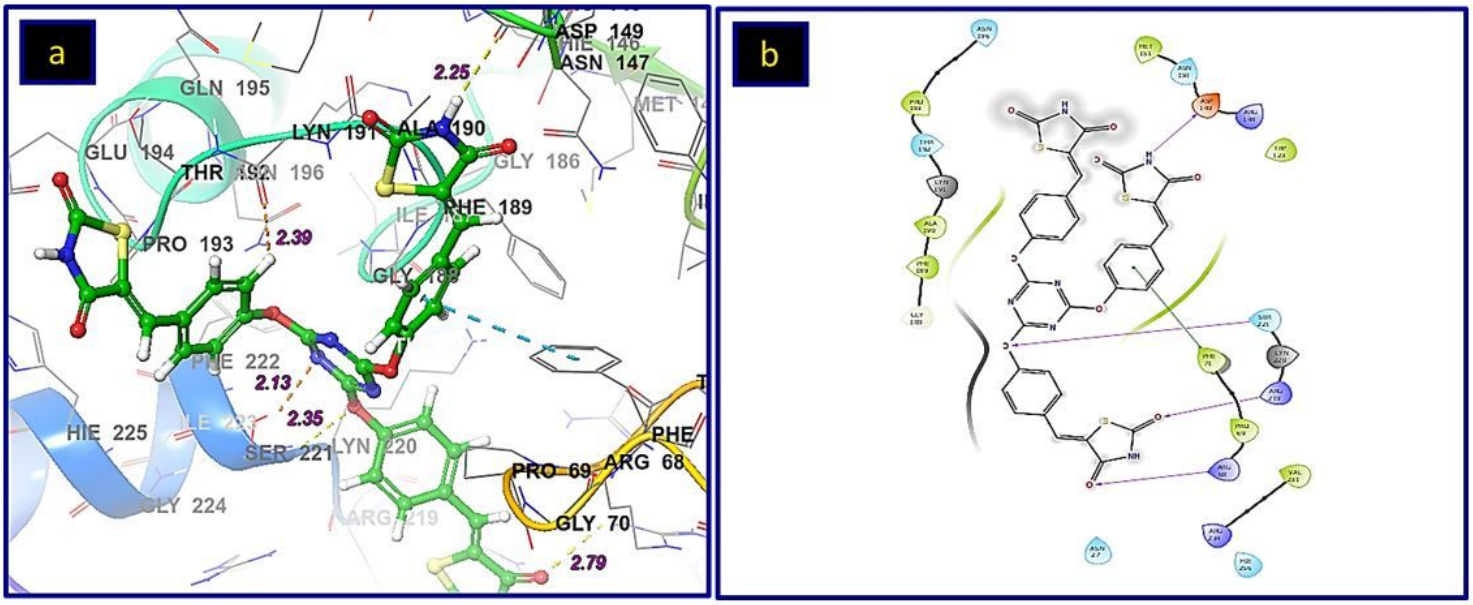

Figure 6

a) The binding mode of **10** ligand with *Bacillus anthracis* (BaDHPS, PDB ID: 3TYE) and **b)** 2D ligand-receptor interaction with 3TYE enzyme

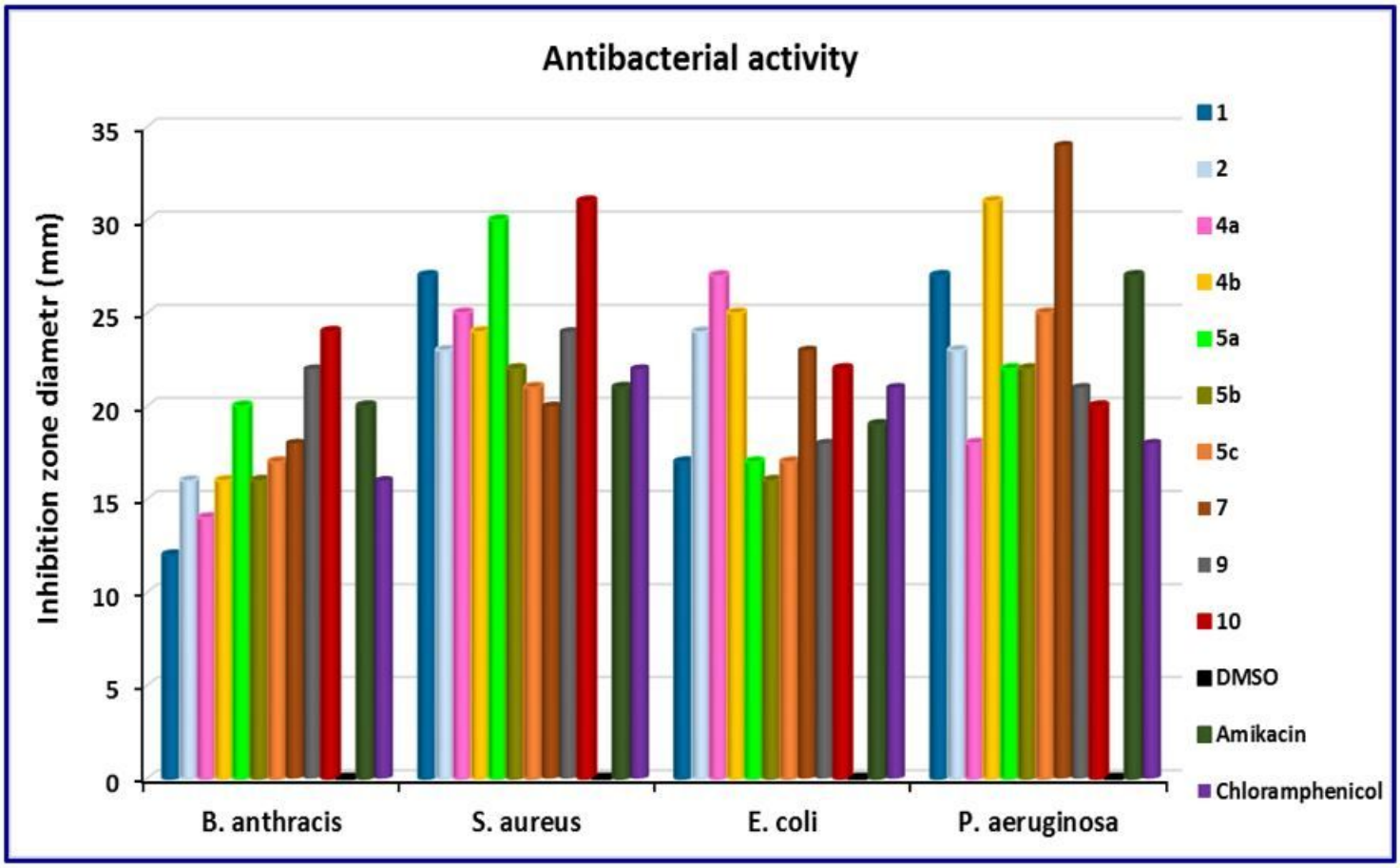

Figure 7

Antibacterial activity of the newly synthesized compounds

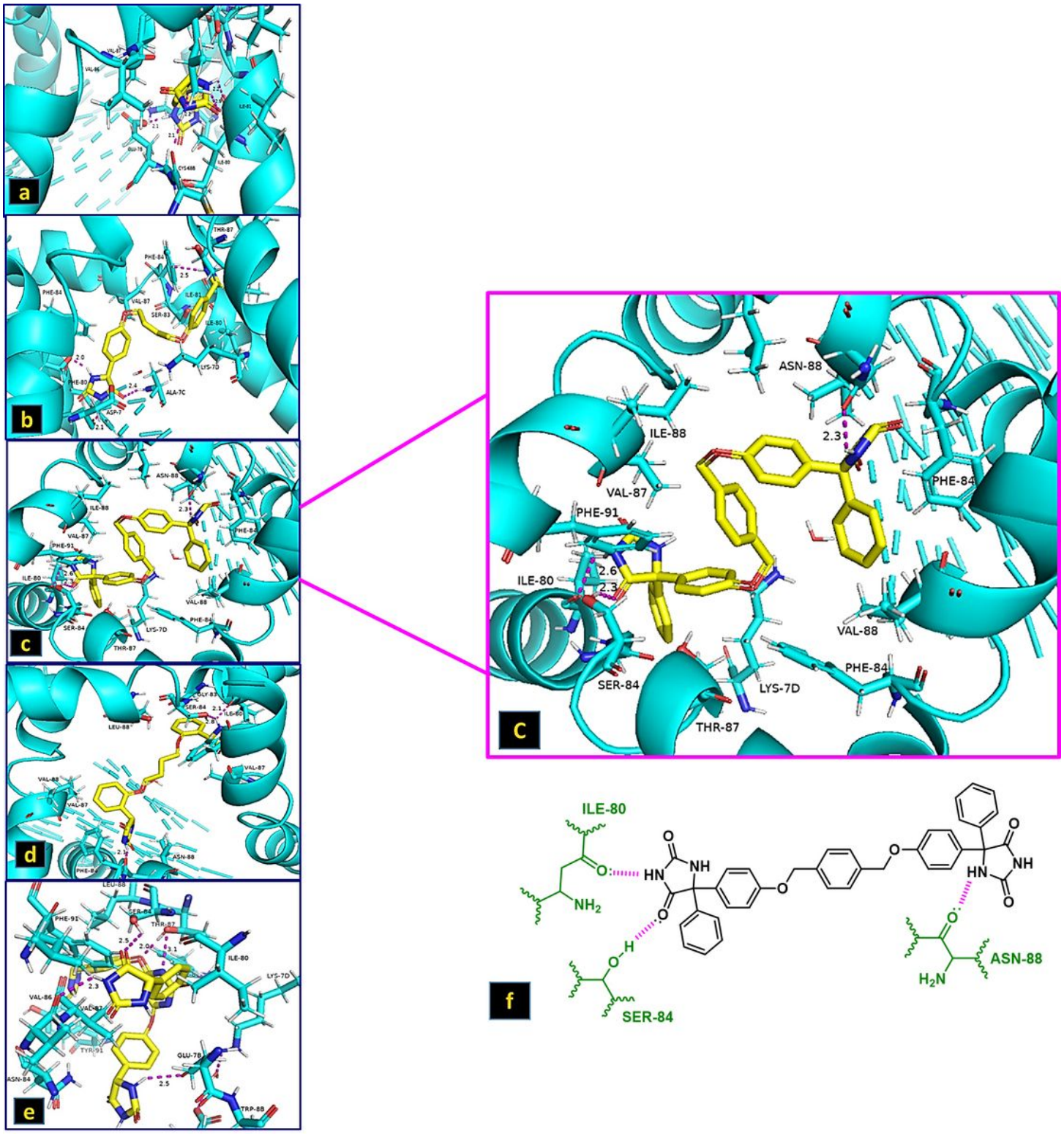

Figure 8

Glide docking model of **IMID-**Compounds consist of (a) **2**, (b) **4b**, (c) **7**, (d) **4a**, (e) **9**, and (f) 2D representations of the binding mode of **7**, respectively through amino acids with different interactions (pink bounds)

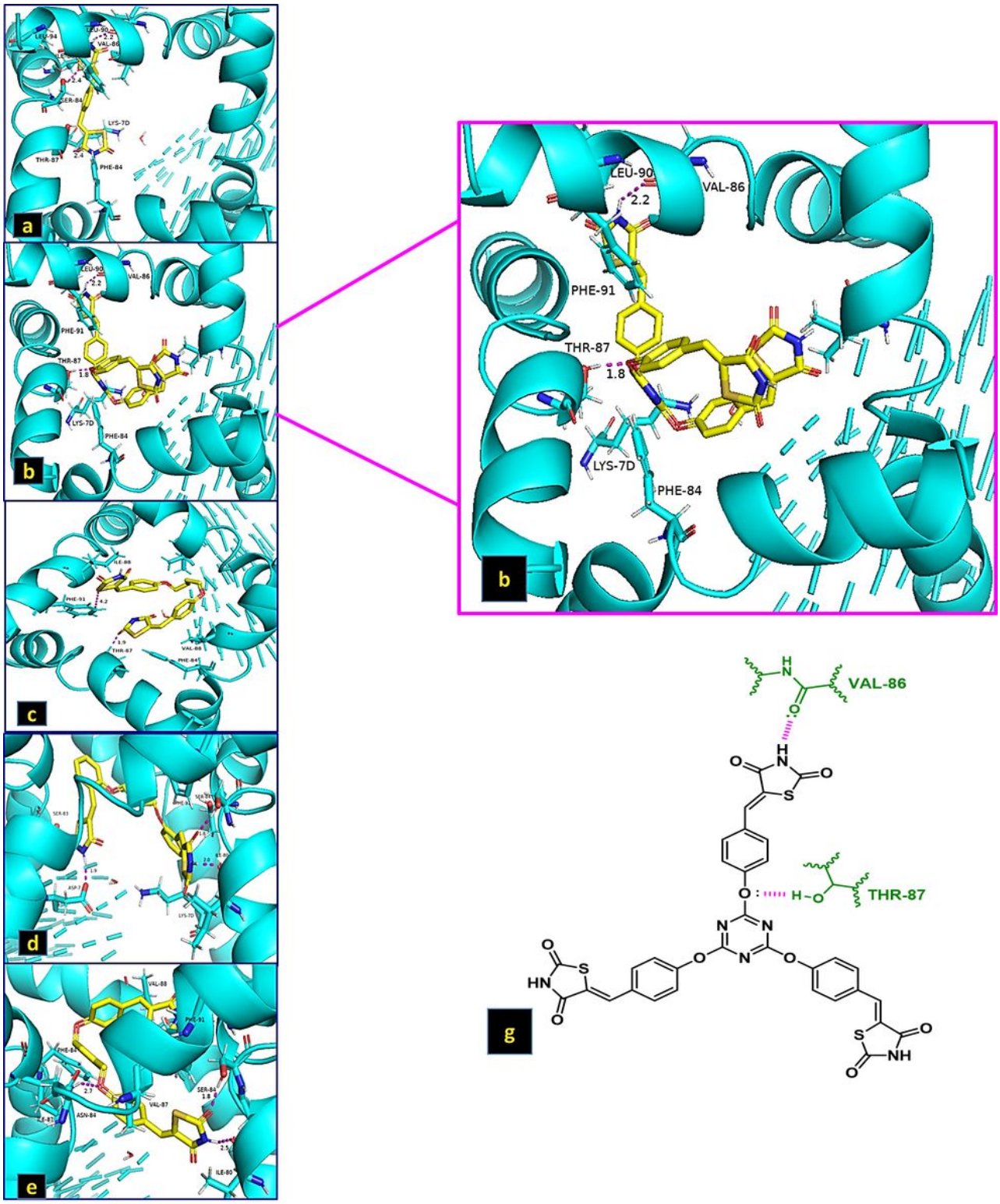

Figure 9

Glide docking model of **TZD**-Compounds consist of (a)**1**, (b)**10**, (c)**5b**, (d)**5a**, (e)**5c**, and (g) 2D representations of the binding mode of **10**, respectively through amino acids with different interactions (pink bounds)

Supplementary Files

This is a list of supplementary files associated with this preprint. Click to download.

- supportingInformations1192023.docx
- scheme1.jpg
- scheme2.jpg
- scheme3.jpg
- scheme4.jpg